Table 1 Derivatives of eigenexponents

Eigenexponent	Analytic solution	Present method	Lu and Murthy's method[2]
$\lambda_{,a}$	1	1	$1 \pm i$
$\lambda_{,b}$	$\pm i$	$\pm i$	$\pm i$

Obviously, the principal eigenexponents and the eigenvector complete sets of $\boldsymbol{K}$ are

$$\lambda = a \pm ib, \qquad \boldsymbol{R} = \boldsymbol{L} = \boldsymbol{I}$$

Hence,

$$\boldsymbol{V}^T(t) = \begin{bmatrix} \cos at \cdot e^{-iat} & b \sin at \cdot e^{-iat} \\ -\dfrac{1}{b} \sin at \cdot e^{iat} & \cos at \cdot e^{iat} \end{bmatrix}$$

$$\boldsymbol{U}(t) = \begin{bmatrix} \cos at \cdot e^{iat} & -b \sin at \cdot e^{-iat} \\ \dfrac{1}{b} \sin at \cdot e^{iat} & \cos at \cdot e^{-iat} \end{bmatrix}$$

By calculation, we have

$$\frac{1}{T}\int_0^T \boldsymbol{v}_1^T \boldsymbol{A}_{,a} \boldsymbol{u}_1 \, \mathrm{d}t = 1 + i, \qquad -\frac{1}{T}\left[\lambda_1 - \boldsymbol{l}_1^T \boldsymbol{A}(0)\boldsymbol{r}_1\right] T_{,a} = -i$$

$$\frac{1}{T}\int_0^T \boldsymbol{v}_2^T \boldsymbol{A}_{,a} \boldsymbol{u}_2 \, \mathrm{d}t = 1 - i, \qquad -\frac{1}{T}\left[\lambda_2 - \boldsymbol{l}_2^T \boldsymbol{A}(0)\boldsymbol{r}_2\right] T_{,a} = i$$

$$\frac{1}{T}\int_0^T \boldsymbol{v}_1^T \boldsymbol{A}_{,b} \boldsymbol{u}_1 \, \mathrm{d}t = i, \qquad -\frac{1}{T}\left[\lambda_1 - \boldsymbol{l}_1^T \boldsymbol{A}(0)\boldsymbol{r}_1\right] T_{,b} = 0$$

$$\frac{1}{T}\int_0^T \boldsymbol{v}_2^T \boldsymbol{A}_{,b} \boldsymbol{u}_2 \, \mathrm{d}t = -i, \qquad -\frac{1}{T}\left[\lambda_2 - \boldsymbol{l}_2^T \boldsymbol{A}(0)\boldsymbol{r}_2\right] T_{,b} = 0$$

Thus, we obtain Table 1.

Obviously, when the period T depends on the parameter to be investigated, Lu and Murthy's method for computing the derivatives of eigenexponents is not applicable. As for the derivatives of the periodic modal matrices, by making use of the analytical method and the present formulas, respectively, we would obtain the same results, as follows:

$$\boldsymbol{H}_a = \begin{bmatrix} it & -tbe^{-i2at} \\ \dfrac{t}{b} e^{i2at} & -it \end{bmatrix}$$

$$\boldsymbol{U}_{,a} = \begin{bmatrix} (-t \sin at + it \cos at)e^{iat} & (-tb \cos at + itb \sin at)e^{-iat} \\ \left(\dfrac{t}{b} \cos at + i\dfrac{t}{b} \sin at\right) e^{iat} & (-t \sin at - it \cos at)e^{-iat} \end{bmatrix}$$

$$\boldsymbol{H}_b = \begin{bmatrix} -\dfrac{1}{b} \sin^2 at & -\sin at \cos at \cdot e^{-i2at} \\ -\dfrac{1}{b^2} \sin at \cos at \cdot e^{i2at} & \dfrac{1}{b} \sin^2 at \end{bmatrix}$$

$$\boldsymbol{U}_{,b} = \begin{bmatrix} 0 & -\sin at \cdot e^{-iat} \\ -\dfrac{1}{b^2} \sin at \cdot e^{iat} & 0 \end{bmatrix}$$

According to Eq. (22), where $\boldsymbol{H}_b = \boldsymbol{V}^T \boldsymbol{U}_{,b}$,

$$\boldsymbol{H}_a = \boldsymbol{V}^T \boldsymbol{U}_{,a}$$

Conclusions

This Note established a key theorem to show that the derivative of a periodic function with respect to the system parameter is generally no longer a periodic function when the period T is dependent on this parameter. A new procedure used to determine the constant $\tilde{c}$ in Eq. (35) has been suggested; it substituted for the periodicity condition given by Eq. (27b) in Ref. 2 during $T_{,p} \neq 0$.

The present generalization preserved all of the advantages of the direct analytical approach, and its effectiveness was demonstrated by an example.

Acknowledgment

This work was supported by the National Natural Science Foundation of China under Grant 19472077.

References

[1] Lim, J. W., and Chopra, I., "Stability Sensitivity Analysis of a Helicopter Rotor," *AIAA Journal*, Vol. 28, No. 6, 1990, pp. 1089–1097.

[2] Lu, Y., and Murthy, V. R., "Sensitivity Analysis of Discrete Periodic Systems with Applications to Helicopter Rotor Dynamics," *AIAA Journal*, Vol. 30, No. 8, 1992, pp. 1962–1969.

[3] Yakubovitch, V. A., and Starzhinskii, V. M., *Linear Differential Equations with Periodic Coefficients*, Vols. 1 and 2, Wiley, New York, 1975.

[4] Dugundji, J., and Wendell, J. H., "Some Analysis Methods for Rotating Systems with Periodic Coefficients," *AIAA Journal*, Vol. 21, No. 6, 1982, pp. 890–897.

[5] Perret-Liaudet, J., "An Original Method for Computing the Response of a Parametrically Excited Forced System," *Journal of Sound and Vibration*, Vol. 196, No. 2, 1996, pp. 165–177.

[6] Erdos, G., and Singh, T., "Stability of a Parametrically Excited Damped Invested Pendulum," *Journal of Sound and Vibration*, Vol. 198, No. 5, 1996, pp. 643–650.

[7] Fung, R. F., Huang, J. S., and Chen, W. H., "Dynamic Stability of a Viscoelastic Beam Subjected to Harmonic and Parametric Excitations Simultaneously," *Journal of Sound and Vibration*, Vol. 198, No. 1, 1996, pp. 1–16.

A. Berman
Associate Editor

Free-Edge Interlaminar Stress Analysis of Composite Laminates by Extended Kantorovich Method

Maenghyo Cho*
Inha University, Inchon 402-751, Republic of Korea
and
Jin-Young Yoon†
Agency for Defense Development, Taejon 305-600, Republic of Korea

I. Introduction

BECAUSE of the mismatch of the elastic properties between plies, serious stress concentration/singularity happens near the free edges of composite laminates, requiring fully three-dimensional stress field modeling. The interlaminar stresses at free edges may cause delamination and laminate failure. Thus, the determination of these stresses is an important issue in the strength analysis and design of laminates.

Exact elasticity solutions for interlaminar stresses with free edges do not exist, and researchers have used analytical and numerical methods. However, accurate and efficient methods that satisfy all of the boundary and interface continuity conditions are rare.

After Spilker and Chou[1] demonstrated the importance of satisfying the traction-free conditions at the edges, stress-based methods were proposed. These methods divide stress functions into in-plane and out-of-plane functions. With appropriate stress function

Received Aug. 20, 1998; revision received Nov. 1, 1998; accepted for publication Dec. 27, 1998.

*Assistant Professor, Department of Aerospace Engineering, 253 Yong-Hyun Dong, Nam-ku. Member AIAA.

†Researcher, 4th R&D Center, Yuseong P.O. Box 35-4.

assumptions, the interlaminar stresses at free edges have been calculated. Kassapoglou and Lagace[2] determined the stresses on the basis of the integrated form of the force and moment equilibriums. However, they assumed that in-plane stresses are constant through the thickness in each ply. The results do not satisfy the pointwise traction-free conditions through the thickness at free edges. Thus, the accuracy of predicted stresses in the out-of-plane direction cannot be guaranteed from this method. Yin[3,4] used piecewise polynomial approximations for the out-of-plane stress functions, and the stresses satisfy the free-edge boundary conditions in the pointwise sense.

Recently, Flanagan[5] proposed an alternative efficient method in which the out-of-plane stress functions were assumed to be the solutions of the free vibration of a clamped–clamped beam. The stress functions given by his approach did not satisfy displacement continuity conditions at the ply interfaces. Thus, the out-of-plane stress distributions are not predicted accurately, and the oscillations appear. In addition, his results cannot recover the classical lamination theory (CLT) solution in the interior of laminates.

In the present study the interlaminar stresses at the free edges in composite laminates are analyzed. The extended Kantorovich method by Kerr[6] is used to predict the accurate stress functions. The Leknitskii stress functions[7] are adopted to divide interlaminar stress expressions into the in-plane and out-of-plane coordinate functions. Under the principle of complementary minimum energy through eigenproblem, the in-plane and out-of-plane stress functions are improved through iteration.

II. Formulation

The geometry of a composite laminate with free edges is given in Fig. 1. The thickness of each ply is the same, and the plies have arbitrary angles relative to the x axis. The laminate is subjected to a mechanical uniaxial extension.

For the given geometric configuration of laminates, the boundary conditions at the free edge and the surfaces of the top and bottom faces are given in Eq. (1):

$$\begin{aligned} &\sigma_2 = \sigma_4 = \sigma_6 = 0 \qquad \text{at} \qquad y = 0, b \\ &\sigma_3 = \sigma_4 = \sigma_5 = 0 \qquad \text{at} \qquad z = \pm h/2 \end{aligned} \tag{1}$$

The laminate is assumed to be in a state of generalized plane strain in the x coordinate. From this assumption and constitutive equations, all of the strains can be expressed in terms of ϵ_1:

$$\epsilon_i = \hat{S}_{ij}\sigma_j + (S_{i1}/S_{11})\epsilon_1 \qquad (i, j = 2, 3, \ldots, 6) \tag{2}$$

where $\hat{S}_{ij} = S_{ij} - (S_{i1}S_{1j}/S_{11})$ and S_{ij} are the components of the transformed compliance matrix.

The coordinates are nondimensionalized as follows:

$$\eta = z/h, \qquad \xi = y/h \tag{3}$$

Leknitskii stress functions are introduced to satisfy the pointwise equilibrium automatically. The interlaminar stress functions can be divided into the in-plane and out-of-plane functions:

$$\begin{aligned} &\frac{\partial^2 F}{\partial \eta^2} = \sigma_2, \qquad \frac{\partial^2 F}{\partial \xi^2} = \sigma_3, \qquad \frac{\partial^2 F}{\partial \eta \partial \xi} = -\sigma_4 \\ &\frac{\partial \Psi}{\partial \xi} = -\sigma_5, \qquad \frac{\partial \Psi}{\partial \eta} = \sigma_6 \end{aligned} \tag{4}$$

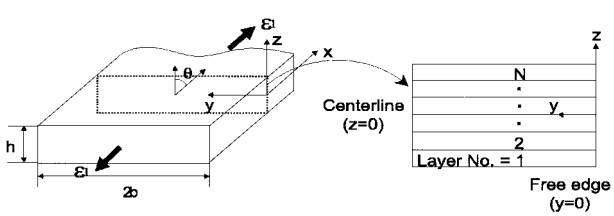

Fig. 1 Geometry of composite laminate with free edge.

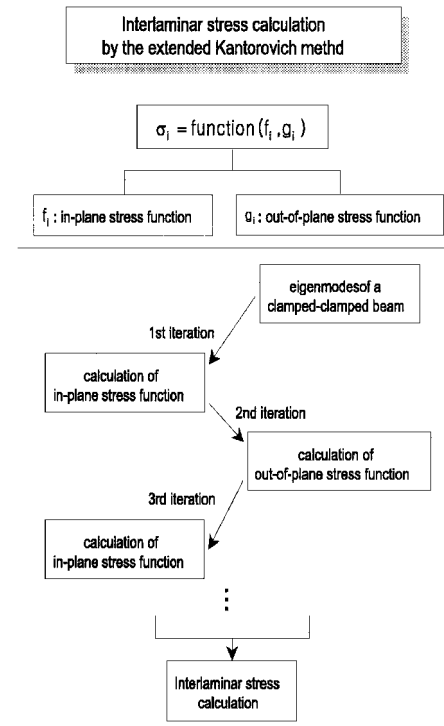

Fig. 2 Schematic procedure by the present method.

where

$$F = \sum_{i=1}^{n} f_i(\xi) g_i(\eta), \qquad \Psi = \sum_{i=1}^{n} p_i(\xi) g_i^I(\eta)$$

The extended Kantorovich method is used to improve in-plane and out-of-plane stress functions through iteration. The schematic procedure is shown in Fig. 2.

First Process: Calculation of In-Plane Stress Functions from Initial Assumption

The in-plane stress functions are determined from the initially assumed basis set of the out-of-plane stress functions. The out-of-plane functions must satisfy the traction-free conditions at the top and bottom surfaces in composite laminates. If the stress functions and their first derivatives are zero in those regions, the preceding conditions are satisfied. The out-of-plane functions $g_i(\eta)$ are assumed as eigenmodes of a clamped–clamped beam per Flanagan.[5]

From the assumed out-of-plane stress functions and the principle of complementary minimum energy, the in-plane stress functions are derived:

$$\delta U = \iint \epsilon_i \delta\sigma_i \, \mathrm{d}y \, \mathrm{d}z = 0 \qquad (i = 2, 3, \ldots, 6) \tag{5}$$

In Eq. (5) the strains are substituted from Eq. (2). Using Eq. (4), the stresses are expressed in terms of f_i and g_i. Equation (5) can be expressed as follows after integration by parts:

$$\begin{aligned} &\int \left[a_{ij}^{(4)} f_j^{IV} + a_{ij}^{(2)} f_j^{II} + a_{ij}^{(0)} f_j + b_{ij}^{(2)} p_j^{II} + b_{ij}^{(0)} p_j + r_i\right]\delta f_i \, \mathrm{d}\xi \\ &+ \int \left[c_{ij}^{(2)} p_j^{II} + c_{ij}^{(0)} p_j + d_{ij}^{(2)} f_j^{II} + d_{ij}^{(0)} f_j + s_i\right]\delta p_i \, \mathrm{d}\xi = 0 \\ &\qquad (i, j = 1, 2, \ldots, n) \end{aligned} \tag{6}$$

where $(r_i, s_i) = \int \epsilon_1 [(S_{12}/S_{11}), (S_{16}/S_{11})] g_i^{II} \, \mathrm{d}\eta$. The detailed expressions of the coefficients $a_{ij}^{(k)}$, $b_{ij}^{(k)}$, $c_{ij}^{(k)}$, and $d_{ij}^{(k)}$ are omitted here because of limited space. The boundary terms induced by integration by parts are eliminated from the condition that g_i and g_i^I are zero at the top and bottom surfaces.

After solving the coupled ordinary differential equations given in Eq. (6), the interlaminar stresses are obtained by the relationships given in Eq. (4):

$$\sigma_2 = \left[v_{ij}^f t_j e^{-\lambda_j \xi} + f_i^{(P)}\right] g_i^{II}(\eta), \qquad \sigma_3 = \lambda_j^2 v_{ij}^f t_j e^{-\lambda_j \xi} g_i(\eta)$$

$$\sigma_4 = \lambda_j v_{ij}^f t_j e^{-\lambda_j \xi} g_i^I(\eta), \qquad \sigma_5 = \lambda_j v_{ij}^p t_j e^{-\lambda_j \xi} g_i^I(\eta) \quad (7)$$

$$\sigma_6 = \left[v_{ij}^p t_j e^{-\lambda_j \xi} + p_i^{(P)}\right] g_i^{II}(\eta)$$

$$(i = 1, 2, \ldots, n) \quad (j = 1, 2, \ldots, 3n)$$

The detailed derivation can be found in Ref. 5.

Second Process: Improvement of Out-of-Plane Stress Functions

The preceding process provides accurate prediction of in-plane stresses (Fig. 3a), but it produces undesirable oscillations in the out-of-plane stresses that are denoted by Flanagan's solution (Fig. 3b). The CLT solutions cannot be recovered in the interior region (Fig. 4). Thus, the one-step process is not adequate for the accurate prediction of the interlaminar stresses.

The extended Kantorovich method is applied to improve the interlaminar stress predictions. By assuming the layer-dependent out-of-plane stress functions in each layer and reapplying the principle of complementary minimum energy, the out-of-plane functions can be improved.

The in-plane stress functions determined from the first process are substituted into the complementary energy density functions. The partial differentiation of g_i is carried out. Because g_i is defined for each layer, the compatibility equations are also obtained in terms of $g_i^{(k)}$ for each layer:

$$\delta U = \int \left[m_{ij}^{(4)(k)} g_j^{(k)IV} + m_{ij}^{(2)(k)} g_j^{(k)II} + m_{ij}^{(0)(k)} g_j^{(k)} + n_i^{(k)}\right] \delta g_i^{(k)} \, \mathrm{d}\eta + \Lambda = 0$$

$$(k = 1, 2 \ldots, N) \quad (i, j = 1, 2, \ldots, n) \quad (8)$$

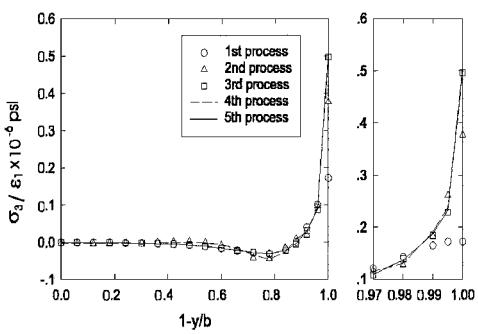

Fig. 3a σ_3 distribution at the 0/90 interface of $[0/90]_S$ laminate under ϵ_1.

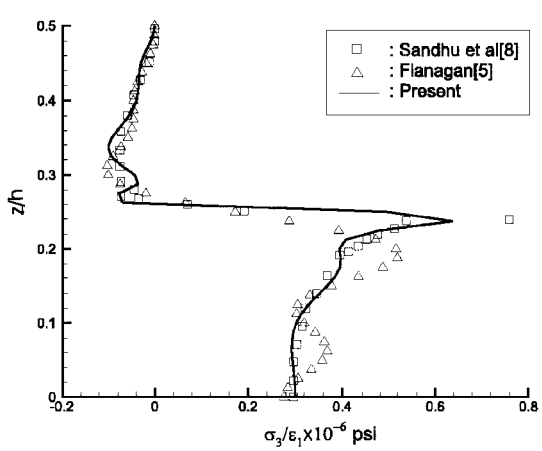

Fig. 3b σ_3 distribution at the free edge of $[0/90]_S$ laminate under ϵ_1.

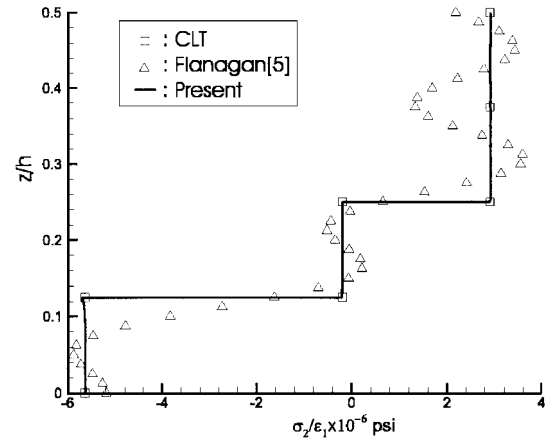

Fig. 4 σ_2 distribution at the interior of $[45/-45/0/90]_S$ laminate under ϵ_1.

where

$$m_{ij}^{(4)(k)} = \int \left[\hat{S}_{22}^{(k)} f_i f_j + \hat{S}_{26}^{(k)} (f_i p_j + p_i f_j) + \hat{S}_{66}^{(k)} p_i p_j\right] \mathrm{d}\xi$$

$$m_{ij}^{(2)(k)} = -\int \left\{\left[2\hat{S}_{23}^{(k)} + \hat{S}_{44}^{(k)}\right] f_i^I f_j^I + \left[\hat{S}_{36}^{(k)} + \hat{S}_{45}^{(k)}\right]\left(f_i^I p_j^I + p_i^I f_j^I\right) + \hat{S}_{55}^{(k)} p_i^I p_j^I\right\} \mathrm{d}\xi$$

$$m_{ij}^{(0)(k)} = \int \hat{S}_{33}^{(k)} f_i^{II} f_j^{II} \, \mathrm{d}\xi, \qquad n_i^{(k)} = \int \epsilon_1 \frac{S_{13}^{(k)}}{S_{11}^{(k)}} f_i^{II} \, \mathrm{d}\xi$$

Λ means boundary terms induced from integration by parts, and the superscript k refers to the kth ply in the laminate.

The homogeneous solutions of $g^{(k)}$ are assumed to be the exponential functions with the eigenvalues $\mu^{(k)}$:

$$g_i^{(k)} = v_i^{g(k)} e^{\mu^{(k)} \eta} \quad (9)$$

Substituting Eq. (9) into Eq. (8), the following equations are obtained:

$$m_{ij}^{(0)(k)} v_j^{g(k)} + \left[m_{ij}^{(2)(k)} + \mu^{(k)^2} m_{ij}^{(4)(k)}\right] v_j^{g^{II}(k)} = 0$$

$$\mu^{(k)^2} v_j^{g(k)} - v_j^{g^{II}(k)} = 0 \quad (10)$$

$$(k = 1, 2, \ldots, N) \quad (i, j = 1, 2, \ldots, n)$$

The positive as well as negative roots of $\mu^{(k)^2}$ are chosen in this process, and the homogeneous solutions are constructed by the $4n$ linear combinations:

$$g_i^{(k)(H)} = v_{ij}^{g(k)} b_j^{(k)} e^{\mu_j^{(k)} \eta}$$

$$(k = 1, 2, \ldots, N) \quad (i = 1, 2, \ldots, n) \quad (j = 1, 2, \ldots, 4n) \quad (11)$$

where $b_j^{(k)}$s are variables to be decided from the boundary and continuity conditions.

The particular solutions $g_i^{(k)(P)}$ are calculated from the assumption that $g_j^{(k)}(\eta)$s are constants in Eq. (8).

The out-of-plane stress functions are given as follows:

$$g_i^{(k)} = g_i^{(k)(H)} + g_i^{(k)(P)}$$

$$(k = 1, 2, \ldots, N) \quad (i = 1, 2, \ldots, n) \quad (12)$$

The variables b_js are determined from the two conditions. First, the out-of-plane stress functions and their first derivatives are zero at the top and bottom surfaces. Second, the boundary terms caused by the integration by parts in Eq. (8) must be zero.

Accordingly, the final interlaminar stresses calculated by the second process are given as follows:

$$\begin{aligned}
\sigma_2 &= f_i(\xi)\left[\mu_j^{(k)^2} v_{ij}^{g(k)} b_j^{(k)} e^{\mu_j^{(k)}\eta}\right] \\
\sigma_3 &= f_i^{II}(\xi)\left[v_{ij}^{g(k)} b_j^{(k)} e^{\mu_j^{(k)}\eta} + g_i^{(k)(P)}\right] \\
\sigma_4 &= -f_i^{I}(\xi)\left[\mu_j^{(k)} v_{ij}^{g(k)} b_j^{(k)} e^{\mu_j^{(k)}\eta}\right] \\
\sigma_5 &= -p_i^{I}(\xi)\left[\mu_j^{(k)} v_{ij}^{g(k)} b_j^{(k)} e^{\mu_j^{(k)}\eta}\right] \\
\sigma_6 &= p_i^{II}(\xi)\left[v_{ij}^{g(k)} b_j^{(k)} e^{\mu_j^{(k)}\eta} + g_i^{(k)(P)}\right] \\
&(i = 1, 2, \ldots, n) \quad (j = 1, 2, \ldots, 4n)
\end{aligned} \tag{13}$$

Third Process: Improvement of In-Plane Stress Functions

The second process eliminated the oscillation of the out-of-plane stress distributions (Fig. 3b). In addition, it recovered the CLT solutions in the interior domain (Fig. 4). However, the interlaminar stresses obtained by the second process still show some oscillations in the in-plane direction as n increases (Fig. 3a).

The iteration process is continued to eliminate these unwanted oscillations. The third iteration procedure is same as that of the first process, except that the out-of-plane stress functions are chosen from the second process.

Further improvement of out-of-plane stress function can be obtained through processes similar to the second process. In-plane stress function can be improved by a process similar to the third one.

III. Numerical Results

For verification, composite laminates are analyzed for various layup configurations. The material properties of a ply are given as follows:

$$E_1 = 20 \times 10^6 \text{ psi}, \qquad E_2 = E_3 = 2.1 \times 10^6 \text{ psi}$$

$$G_{12} = G_{13} = G_{23} = 0.85 \times 10^6 \text{ psi}$$

$$\nu_{12} = \nu_{13} = \nu_{23} = 0.21$$

The in-plane length b is assumed to be $2h$.

To examine convergence, four iterations were completed. The second and fourth processes generated stress oscillations along the in-plane direction. The first and third processes generated the fluctuation of stresses through the thickness. However, these oscillations decreased rapidly upon further iteration. Through numerical examples the interlaminar stresses almost converge to the expected values with only the two-time iteration process (Fig. 3a).

The results in all of the figures after Fig. 3a are obtained with three-time iterations with $n = 8$. The in-plane and out-of-plane stress distributions are given, and they are compared with previous results. In the figures, Flanagan's results are equivalent to those of the first process.

Uniaxial Tension

Figure 3a shows the σ_3 distribution at the 0/90 interface of the $[0/90]_S$ laminate under ϵ_1. The plot shows the results as the iteration continues. The result of the third process converges to a consistent value and agrees with Flanagan's results except at the free edge. As mentioned in the preceding section, the result obtained by the second process oscillates. The peak stress at the free edge is significantly improved by the present method. The distribution of σ_3 at the free edge in the $[0/90]_S$ laminate is shown in Fig. 3b. For comparison Sandhu's result[8] is shown as well. Sandhu's result was obtained by the finite element method using 288 continuous traction elements. The new results agree with those of Sandhu, and the stress singularity at the interface is predicted well.

The distribution of σ_2 at the interior of the $[45/-45/0/90]_S$ laminate (Fig. 4) shows that the present method recovers the CLT solution exactly without any oscillation, whereas Flanagan's method does not.

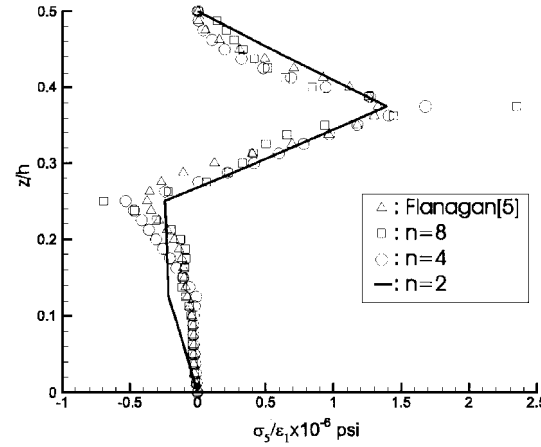

Fig. 5 σ_5 distribution at the free edge of $[45/-45/0/90]_S$ laminate for various numbers of stress functions under ϵ_1.

Interlaminar Stresses for Various Numbers of Stress Base Functions

The preceding results were obtained for $n = 8$. They provide very accurate interlaminar stress predictions. Even for a smaller number of stress base functions, convergent solutions can be obtained within three iterations.

Figure 5 shows the interlaminar shear stress σ_5 along the in-plane and out-of-plane directions after three different iterations. In the case of $n = 2$, the interlaminar stresses are close to those of $n = 8$ in the interior zones. However, near the free edges interlaminar stresses in the case of $n = 2$ are less accurate than those of $n = 8$. The analysis with a small number of base functions ($n = 2$) offers computational efficiency and accuracy comparable to those of the previously reported results.[2,4,5] For the accurate stress predictions a large number of initial stress base functions is required ($n = 8$). However, for reasonable stress predictions, a small number of stress base functions ($n = 2$) is sufficient.

IV. Conclusions

The interlaminar stresses near free edges in composite laminates have been analyzed by the extended Kantorovich method. Through the iteration process the accurate interlaminar stresses are obtained. The high stress gradient at the free edge correlated well with the previous results, and the position of maximum stress was predicted accurately. The CLT solution was recovered at the interior of laminates. Therefore, the new method accurately predicts the stress distributions over the whole domain of laminates.

In the given numerical examples, four time iterations were performed. However, the calculation process is not complicated because it requires only two iterative steps that consist of a process to calculate the out-of-plane stress functions from in-plane functions and vice versa.

Numerical examples demonstrated that the present method provides reliable prediction of free-edge interlaminar stresses for various layup configurations under extensional loadings.

Acknowledgment

This research was supported by the 1996 Korea Science and Engineering Foundation (KOSEF 961-1003-027-1). The authors gratefully acknowledge this support.

References

[1] Spilker, R. L., and Chou, S. C., "Edge Effects in Symmetric Composite Laminates: Importance of Satisfying the Traction-Free-Edge Condition," *Journal of Composite Materials*, Vol. 14, Jan. 1980, pp. 2–20.

[2] Kassapoglou, C., and Lagace, P. A., "An Efficient Method for the Calculation of Interlaminar Stresses in Composite Materials," *Journal of Applied Mechanics*, Vol. 53, Dec. 1986, pp. 744–750.

[3] Yin, W. L., "Free-Edge Effects in Anisotropic Laminates Under Extension, Bending and Twisting. Part 1—A Stress Function Based Variational

Approach," *Journal of Applied Mechanics*, Vol. 61, June 1994, pp. 410–415.

[4]Yin, W. L., "Free-Edge Effects in Anisotropic Laminates Under Extension, Bending and Twisting. Part 2—Eigenfunction Analysis and the Results for Symmetric Laminates," *Journal of Applied Mechanics*, Vol. 61, June 1994, pp. 416–421.

[5]Flanagan, G., "An Efficient Stress Function Approximation for the Free-Edge Stresses in Laminates," *International Journal of Solids and Structures*, Vol. 31, No. 7, 1994, pp. 941–952.

[6]Kerr, A., "An Extended Kantorovich Method for the Solution of Eigenvalue Problems," *International Journal of Solids and Structures*, Vol. 5, 1969, pp. 559–572.

[7]Lekhnitskii, S. G., *Theory of Elasticity of an Anisotropic Body*, Holden–Day, San Francisco, 1963, Chap. 3.

[8]Sandhu, R. S., Wolfe, W. E., Sierakowski, R. L., Chang, C. C., and Chu, H. R., "Finite Element Analysis of Free-Edge Delamination in Laminated Composite Specimens," U.S. Air Force Wright Lab., Rept. WL-TR-91-3022, 1991.

R. K. Kapania
Associate Editor

Synthesis Technique for the Nonclassically Damped Structures Using Real Schur Vectors

Jinwu Xiang*
Beijing University of Aeronautics and Astronautics, 100083 Beijing, People's Republic of China
and
Gexue Ren† and Qiuhai Lu‡
Tsinghua University, 100084 Beijing, People's Republic of China

Introduction

WITH the extensive application of composite materials and energy-dissipative devices in engineering structures, dynamic analyses of nonclassically damped systems are now frequently found. For damped systems, Foss[1] has proposed what is commonly known as the complex mode theory. Caughey and O'Kelly,[2] Liu and Wilson,[3] and Caughey and Ma[4] have given the conditions under which the damped systems can be decoupled with the real modes in physical space or configuration space. In practice, the verification of those conditions is often prohibitive due to the size of the problem and numerical difficulty. Thus, in general, the use of complex modes theory in state space is the practice. The complex mode theory is actually based on Jordan decomposition, where numerical difficulties arise under defectiveness conditions.[5,6] Zheng et al.[7] and Ren and Zheng[8,9] proposed the quasidecoupling technique, which is based on real Schur's decomposition instead of on Jordan's decomposition. Distinctive to the complex mode theory, the quasidecoupling approach involves only orthogonal operations, indiscriminately applied to defective and nondefective systems and uses only one side of the invariant space. The difference between Jordan's decomposition and Schur's decomposition lies in the adoption of the bases of the invariant subspace. The adoption of complex eigenvectors results in the complex mode theory with the diagonal form or Jordan form (defective cases) as the canonical form. On the other hand, the adoption of the real Schur vectors results in the quasidecoupling approach, with the real Schur form as the canonical form.

Received June 3, 1998; revision received Oct. 27, 1998; accepted for publication Jan. 20, 1999.

*Associate Professor, Department of Aircraft Design and Applied Mechanics.
†Associate Professor, Department of Engineering Mechanics.
‡Lecturer, Department of Engineering Mechanics.

Following decades of development, the mode synthesis technique is now widely used in engineering applications, with its theoretical foundation solidly established. The mode synthesis technique for nonproportionally or nonclassically damped systems has also been developed by many researchers[10–12] and may generally be classified into two categories: those that use real modes and those that use complex modes. It has been agreed that, if real modes are used in the synthesis, off-diagonal elements of the transformed damping should be reserved for better damping synthesis.[10] When using the complex mode synthesis in state space, the effects of the off-diagonal elements in the real mode case are automatically taken into consideration because of the biorthogonality of the complex constraint dynamic modes. From the present understanding of the principles of mode synthesis, it is the subspace spanned by the modes used in the synthesis that is of the essence, not the modes themselves. Based on these arguments, whereas the complex modes were used in the mode synthesis technique, the real Schur vectors spanning the same invariant subspace can be used in replacement. This Note tries to use the real Schur vectors in the mode synthesis technique for nonclassically damped systems. For conciseness and because of limitations on the size of this Note, the work is carried out in the fixed interface method.

Substructure Analysis with Arnoldi Reduction and the Real Schur Decomposition

The proposed component mode synthesis is illustrated with two substructures. The governing equation of the damped substructures can be written as

$$\begin{bmatrix} m^s_{ii} & m^s_{ij} \\ m^s_{ji} & m^s_{jj} \end{bmatrix} \begin{bmatrix} \ddot{x}^s_i \\ \ddot{x}^s_j \end{bmatrix} + \begin{bmatrix} c^s_{ii} & c^s_{ij} \\ c^s_{ji} & c^s_{jj} \end{bmatrix} \begin{bmatrix} \dot{x}^s_i \\ \dot{x}^s_j \end{bmatrix} + \begin{bmatrix} k^s_{ii} & k^s_{ij} \\ k^s_{ji} & k^s_{jj} \end{bmatrix} \begin{bmatrix} x^s_i \\ x^s_j \end{bmatrix} = \begin{bmatrix} f^s_i(t) \\ f^s_j(t) \end{bmatrix} + \begin{bmatrix} 0 \\ f^s_{12}(t) \end{bmatrix} \tag{1}$$

where superscript s is the index of substructures and subscripts i and j are the indices of the variables corresponding to the internal degrees of freedom (DOFs) and interface DOFs, respectively. In Eq. (1), m^s_{ab}, c^s_{ab}, and k^s_{ab} $(a, b = i, j; s = 1, 2)$ are the mass matrix, damping matrix, and stiffness matrix partitions corresponding to the internal/external DOFs. The nonsymmetric damping matrix is allowed in this research as in the case of damped structures with Coriolis effects, e.g., rotating helicopter rotor systems. Also, f^s_i and f^s_j are the external forces acting on the internal DOFs x^s_i and the interface DOFs x^s_j, respectively. Here, f^s_{12} is the interface force satisfying

$$f^1_{12} + f^2_{12} = 0 \tag{2}$$

By rewriting the governing equation (1) and the equilibrium equation (2) of the interface forces in state-space form, we have

$$\begin{bmatrix} A^s_{ii} & A^s_{ij} \\ A^s_{ji} & A^s_{jj} \end{bmatrix} \begin{bmatrix} \dot{y}^s_i \\ \dot{y}^s_j \end{bmatrix} + \begin{bmatrix} B^s_{ii} & B^s_{ij} \\ B^s_{ji} & B^s_{jj} \end{bmatrix} \begin{bmatrix} y^s_i \\ y^s_j \end{bmatrix} = \begin{bmatrix} F^s_i(t) \\ F^s_j(t) \end{bmatrix} + \begin{bmatrix} 0 \\ F^s_{12}(t) \end{bmatrix} \tag{3a}$$

$$F^1_{12} + F^2_{12} = 0 \tag{3b}$$

where

$$A^s_{ab} = \begin{bmatrix} c^s_{ab} & m^s_{ab} \\ -m^s_{ab} & 0 \end{bmatrix}, \qquad B^s_{ab} = \begin{bmatrix} k^s_{ab} & \\ & m^s_{ab} \end{bmatrix}$$

$$y^s_a = \begin{bmatrix} x^s_a \\ \dot{x}^s_a \end{bmatrix}, \qquad F^s_a = \begin{bmatrix} f^s_a \\ 0 \end{bmatrix}, \qquad F^s_{12} = \begin{bmatrix} f^s_{12} \\ 0 \end{bmatrix}$$

The fixed interface modes are usually defined as one set of the independent bases of the lower invariant subspace of the interface-fixed substructure. In this Note, the orthogonal bases of the invariant subspace of the interface fixed substructures are adopted, i.e., the invariant subspace of the following eigenproblem:

$$\lambda A^s_{ii} Y^s_i + B^s_{ii} Y^s_i = 0 \tag{4}$$